RSC Advances

PAPER

Cite this: *RSC Adv.*, 2016, **6**, 102831

Differential *in vitro* and *in vivo* anti-angiogenic activities of acetal and ketal andrographolide derivatives in HUVEC and zebrafish models†

Dekuan Sheng,‡[a] Jingjing Li,‡[b] Kun Wang,‡[a] Yuran Peng,[a] Shang Li,[b] Yicheng Sun,[a] Zhuyun Liu,[a] Decai Wang,[a] Simon Ming Yuen Lee*[b] and Guo-Chun Zhou*[a]

A series of acetal and ketal derivatives of andrographolide were synthesized and their anti-angiogenic activities were tested *in vitro* and *in vivo* using HUVEC and zebrafish models, respectively. These compounds exhibited better angiogenesis inhibitory activity in both models than the parent compound andrographolide (**1**). The compounds' SARs differed for the HUVEC and zebrafish models, in that 14α-ketal **2** showed the best activity for *in vivo* anti-angiogenesis in zebrafish while 14α-acetals **4**, **5** and **6** had greater *in vitro* anti-angiogenic activity with HUVECs than the other compounds and **1**. The results suggested that methylene acetals **4**, **5** and **6** were possibly hydrolyzed into **3** or **1** in zebrafish and that 14α-ketal **2** probably did not fully act as a pro-drug of **3** or **1** in zebrafish, instead exerting the anti-angiogenic effect itself or being metabolized into an unknown more active form(s) than **3** and **1** to block *in vivo* angiogenesis in zebrafish. The underlying molecular mechanisms of compound **2**'s action were explored and the results indicated that VEGF-stimulated angiogenesis was significantly inhibited by compound **2** *via* targeting the phosphorylation of VEGFR2 and VEGFR2-mediated downstream angiogenesis signaling pathways. Therefore, this report demonstrates that andrographolide derivative(s) can be developed into therapeutic agent(s) against excessive angiogenesis, including tumor angiogenesis, after further improvement of the potency and stability of this series of andrographolide derivatives.

Received 29th June 2016
Accepted 8th October 2016

DOI: 10.1039/c6ra16758f

www.rsc.org/advances

Introduction

Traditional or folk medicines are widely used in many countries' primary healthcare and some of them have been applied to treat diseases for thousands of years. Even in the modern world, the utilization of natural products for drug discovery and development is actually still active and promising; for example, a recent report[1] shows that 49% of 175 small molecules approved for cancer-related applications up to the end of 2014 are either natural products or directly derived from natural products. Andrographolide (**1**), defined as a "heat-clearing and detoxifying" agent in Chinese Traditional Medicine,[2] is a labdane-type diterpene and representative active ingredient of *Andrographis paniculata* (Burm.f.) Nees. Even though **1** is a polyol and obeys the "Rule of Five", both its water-solubility and lipo-solubility are very poor (it is insoluble in water, soluble in boiling ethanol, almost insoluble in ether, and only slightly soluble in chloroform, methanol and ethanol at room temperature), leading to weak potency and limited therapeutic efficacy. However, since **1** possesses an interesting pharmacophore that exerts various pharmacological activities and has therapeutic potential for a wide range of diseases,[2,3] a lot of andrographolide derivatives and their pharmacological activities have been reported in recent years to improve its physiochemical properties and pharmaceutical features.[4]

Angiogenesis plays an important role from early in embryogenesis, when it is involved in the growth of new vessels, to adulthood, when revascularization of tissues is necessary for their recovery from ischemic injury. Unlike the adjustable, controllable and balanced angiogenic activity in the normal adult organism, the regulatory mechanisms of angiogenesis in an active tumor are destroyed by overgrowing cancer cells.[5] Excessive activation of angiogenesis is the basal pathological process for fast tumor progression and metastasis;[6] therefore, starving cancer cells *via* blockade of angiogenesis by targeting activated endothelial cells is an important cancer chemotherapy.[7] Since endothelial cells are responsible for the basic processes of *in vitro* angiogenesis, for example, proliferation, migration, invasion and tube formation,[8] *in vitro* anti-

[a]*School of Pharmaceutical Sciences, Nanjing Tech University, Nanjing 211816, Jiangsu, China. E-mail: gczhou@njtech.edu.cn; Tel: +86-25-58139415*

[b]*State Key Laboratory of Quality Research in Chinese Medicine, Institute of Chinese Medical Sciences, University of Macau, Macao, China. E-mail: simonlee@umac.mo; Tel: +86-53-88224695*

† Electronic supplementary information (ESI) available: Fig. S1–S11, Table S1, NMR spectra and HPLC spectra of compounds **2**, **4**, **5**, **6** and **9** in PDF format. See DOI: 10.1039/c6ra16758f

‡ These authors contributed equally to this paper.

angiogenesis drug discovery is conducted by inhibiting these essential functions of endothelial cells. Vascular endothelial growth factor (VEGF) is one of the major regulators of the expansion of the vascular tree[9] and acts by binding VEGFR2 to transduce the angiogenic signals. The important outcome of VEGF stimulation is the tyrosine phosphorylation of VEGFR2, which initiates angiogenic functions of blood endothelial cells,[10] leading to the activation of downstream signaling cascades[11] such as mitogen-activated protein kinase (MEK), extracellular signal-regulated kinase 1 and 2 (ERK1/2), *etc.* Therefore, the suppression of the VEGF/VEGFR2 signaling pathway is considered to be an important strategy for angiogenesis inhibition. Meanwhile, as it was demonstrated that many anti-angiogenic drugs elicit similar responses in the zebrafish (*Danio rerio*) model to those observed in mammalian systems,[12] zebrafish embryos have been used as a live *in vivo* model of angiogenesis in addition to the endothelial cell model of *in vitro* angiogenesis in angiogenesis-related drug discovery. Furthermore, transgenic zebrafish expressing enhanced green fluorescent protein (GFP) in their vasculature have allowed observations of the responses of live embryos to drugs in real time.[13] We have previously used the zebrafish model for the study of natural products as anti-angiogenesis[14] or pro-angiogenesis[15] agents and for the structure–activity relationship (SAR) analysis of anti-angiogenesis activity and toxicity.[16]

With our aim of searching for small molecular entities with anti-angiogenesis activity, we investigated andrographolide derivatives. Even though the applications of andrographolide (**1**) as a traditional medicine mainly focused on its anti-infection and anti-inflammation efficacy to relieve internal heat in the clinic trial,[2] there are some reports[17] demonstrating the anti-angiogenic activity of andrographolide and its derivatives, which inhibited retinal angiogenesis, hepatic angiogenesis, and tumor angiogenesis. In this paper, we report the synthesis and discovery of 14-acetal or 14-ketal derivatives of andrographolide as anti-angiogenic agents. Importantly, it is disclosed that the anti-angiogenic activity of compounds **2**, **3**, **4**, **5**, **6** and **9** differed depending on whether they were tested using the *in vitro* human umbilical vein endothelial cell (HUVEC) model or *in vivo* zebrafish model. The 14α-acetals **4**, **5** and **6** exhibited better *in vitro* anti-angiogenic activity with the HUVEC model, but 14α-ketal **2** demonstrated the highest anti-angiogenic activity when applied *in vivo* on zebrafish. In addition, the underlying molecular mechanisms of compound **2**'s action were explored and the results indicated that VEGF-stimulated angiogenesis was significantly inhibited by compound **2** *via* targeting the phosphorylation of VEGFR2 and VEGFR2-mediated downstream angiogenesis signaling pathways. This report paves a new route towards andrographolide derivative(s) that can be developed into therapeutic agent(s) against excessive angiogenesis including tumor angiogenesis.

Results and discussion

Synthesis of acetals and ketals of andrographolide

Our pilot work set out to improve the lipo-solubility of andrographolide (**1**), and we were interested in introducing acetal or/and ketal to the 3, 14 and 19 positions in **1** to form possible pro-drugs of **1** or **3**. The synthesis of target acetal and ketal compounds is described in Scheme 1 and, as envisaged, all of these compounds actually have excellent lipo-solubility in alcohols, ethers, ethyl acetate, dichloromethane (DCM), chloroform *etc.*, although **1** (clog $P = 2.1186$) addresses the "Rule of Five" criteria more fully than the other compounds (clog P values are listed in Scheme 1). The improved lipo-solubility of these derivatives makes them much more convenient for drug applications than andrographolide (**1**), which is poorly water- and lipo-soluble. In addition, better lipo-solubility could increase cell permeability of molecules to improve drug delivery and utilization.

Starting from andrographolide (**1**), compounds **2** and **3**[4h] were formed in different ratios as the reaction conditions were changed (Table 1), for example, only about 4% yield of 14α-ketal **2** was given using 5.8 equiv. of dimethoxypropane (DMP) in DCM under normal reaction conditions (Method A, Table 1) as for our previously reported procedures.[4h] Increasing DMP to more than 14 equiv. enhanced the yield of **2** to 40% (Method B, Table 1); however, it was discovered that the reaction only gave a 34% yield of **2** and the total yield of **2** and **3** sharply decreased if 28 equiv. of DMP was used as a reactant and a solvent (Method C, Table 1), suggesting that the optimal dilution by DCM is helpful for the reaction. Then, according to our previously reported procedures,[4h] a 14-epimer (**8**)[4h] of andrographolide was prepared from **3** *via* compound **7**[4h] by Mitsunobu reaction and hydrolysis. Likewise, using synthetic methods similar to those for the synthesis of **2**, 14β-ketal compound **9**, as a 14-epimer of **2**, was prepared from starting material **8** with yields similar to those of **2** under the varying reaction conditions (Table 1).

Considering that a methylene acetal has less hindrance and is chemically more stable than a ketal, which could affect its

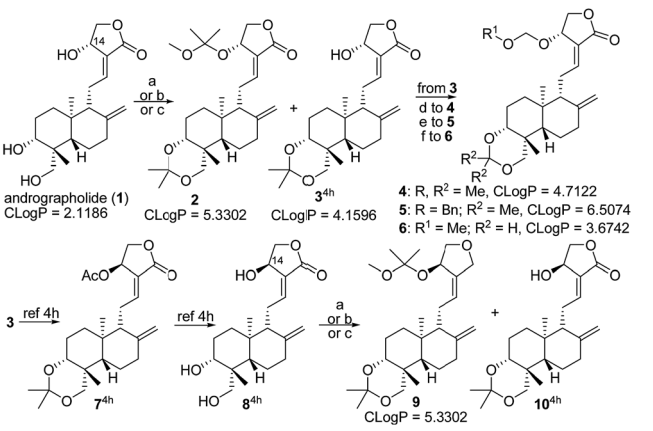

Scheme 1 Synthesis of acetal and ketal derivatives of andrographolide. Reagents and reaction conditions: (a) Method A: modified from ref. 4*h*, 5.8 equiv. DMP, DCM (1/2 v/v DCM/DMP), 45 °C. (b) Method B: 14 equiv. DMP, DCM (2/5 v/v DCM/DMP), 45 °C. (c) Method C: 28 equiv. DMP, w/o DCM, 45 °C. (d) MOMCl, DCM, DIPEA, at 0 °C for 20 min and at 35 °C for 50 h. (e) BOMCl, DCM, DIPEA, 0 °C for 20 min, and then 35 °C for 48 h. (f) MOMCl, DCM, TEA, rt, 12 h. clog P values representing the partition coefficient (octanol/water) were calculated from Chem3D Ultra 8.0.

Table 1 Relationship between ratios of reactants with proportions of two products[a]

Method	1 or 8 (equiv.)	DMP (equiv.)	DCM/DMP (v/v)	Yield[b] (%) 2/9	3/10
A	1	5.8	1/2	4/3	93/90
B	1	14	2/5	40	56
C	1	28.3	w/o DCM	38	48

[a] Reactions were catalyzed by 10 equiv.% of PPTS and conducted at 45 °C bath temperature. [b] Isolated yield.

activity, 14-methylene acetal compounds **4**, **5** and **6** were also synthesized. Under standard conditions using diisopropyl ethyl amine (DIPEA) as a base, 3,19-acetonylidene-14α-acetals **4** and **5** were afforded by the reaction of **3** with chloromethyl methyl ether (MOMCl) and chloromethylbenzyl ether (BOMCl), respectively. Interestingly, when triethylamine (TEA) was applied as a base, 3,19-methylene acetal-14α-methylene acetal **6** was generated by the reaction of **3** with MOMCl, such that the 3,19-acetonylidene ketal was removed and replaced by the chemically more stable 3,19-methylene acetal.

Determination of anti-angiogenic activity in zebrafish

As the observation of vasculature development in zebrafish to determine *in vivo* angiogenesis is becoming an acceptable and reliable angiogenesis model,[12,13] 24 hour post fertilization (hpf) transgenic zebrafish embryos, *Tg(fli-1a:EGFP)y1*, were used to evaluate the *in vivo* anti-angiogenic activity of these ketals and acetals.

Inter-segmental vessels (ISVs) sprouting and elongating from the dorsal aorta (DA) and posterior cardinal vein (PCV) to form the adjoining dorsal lateral anastomotic vessels (DLAVs) were defined as intact. On the other hand, ISVs sprouting from DA or PCV but not forming complete ISVs were defined as defective. Embryos with any incomplete ISVs were defined as displaying an anti-angiogenic phenotype. As shown in Fig. S1 (ESI†), after 24 hpf zebrafish embryos were treated with a vehicle, the positive control drug VRI (250 ng ml^{-1}) and 30 μM of the tested compounds for 12 h, intact ISVs were observed in the vehicle control group and defective ISVs revealed an anti-angiogenic phenotype in the VRI-treated group and some drug-treatment groups (a white asterisk indicates ISVs loss). It was found that ketal compound **2** showed the strongest *in vivo* anti-angiogenic activity in the zebrafish model of all of the compounds.

As shown in Fig. 1, after the 24 hpf embryos were exposed to various concentrations (10, 30 and 100 μM) of **2** for 12 h, the formation of ISVs showed different growth inhibition and the overall percentage of zebrafish embryos with the anti-angiogenic phenotype increased dose-dependently compared to the vehicle control group. The IC_{50} values based on quantitative analysis of the effect of these tested compounds on blood vessel loss (Fig. 1 and S2 in ESI†) are shown in Table 2.

Firstly, it was found that up to 300 μM of parent compound **1** just weakly inhibited zebrafish embryos' blood vessel formation (entry 1, Table 2). 14α-Compound **2** possessed the best anti-

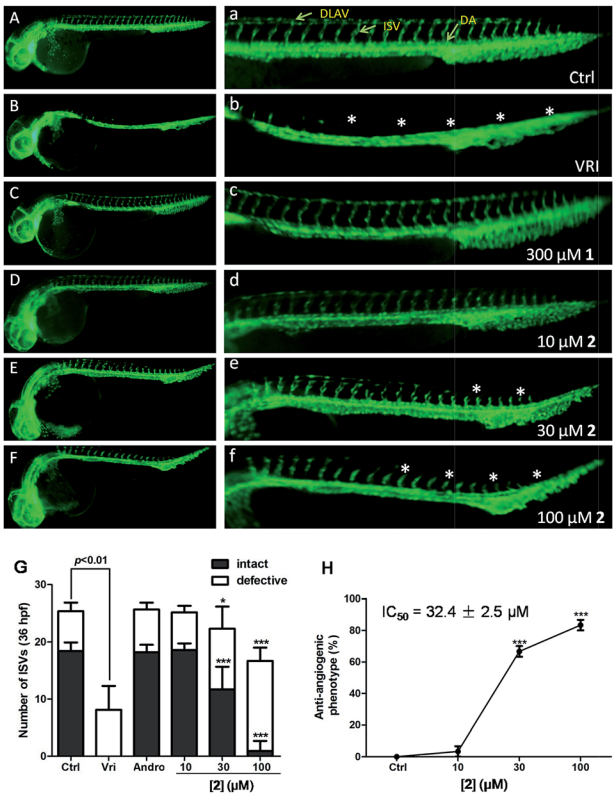

Fig. 1 The *in vivo* anti-angiogenic effects of ketal **2** on *Tg(fli-1a:EGFP)y1* zebrafish (white asterisks in (b), (e) and (f) indicated ISVs loss).

angiogenic activity in terms of the formation of zebrafish embryos' blood vessels (entry 2, Table 2). As shown in Fig. 1(G and H), more than 60% of zebrafish embryos exhibited defects in angiogenesis after treatment with 30 μM of **2** for 12 h compared to the vehicle control group, whereas its 14β-isomer **9** was almost inactive (entry 7, Table 2), indicating that 14-stereochemistry is important for the compounds' *in vivo* anti-angiogenic activity in zebrafish. Meanwhile, compounds **3**, **4** and **5** exhibited similar inhibitory activity towards zebrafish embryos' blood vessel formation (entries 3, 4 and 5, Table 2), suggesting that if the potency of **3**, **4** and **5** was not coincidently identical, it was possible for 14α-methylene acetals **4** and **5** to act as pro-drugs of **3**. Compared to 3,19-acetonylidene ketal **4**, 3,19-methylene acetal **6** totally lost its anti-angiogenic activity

Table 2 Anti-angiogenic results of these compounds in the *in vivo* zebrafish model and the *in vitro* HUVEC model

Entry	Cmpd	IC_{50} (μM) Against zebrafish	Against HUVEC
1	**1**	>300	67.6 ± 6.0
2	**2**	32.4 ± 2.5	18.7 ± 0.8
3	**3**	98.7 ± 3.3	16.6 ± 1.2
4	**4**	103.9 ± 5.9	4.7 ± 0.9
5	**5**	99.1 ± 3.5	5.7 ± 1.3
6	**6**	>300	6.9 ± 0.4
7	**9**	>300	22.4 ± 3.9

(entry 6, Table 2), illustrating the importance of 3,19-acetonylidene ketal to *in vivo* angiogenesis inhibition in the zebrafish model. Combining these activity results for **3**, **4**, **5** and **6** in the zebrafish model, we can hypothesize that these methylene acetals of **4**, **5** and **6** were (biologically) unstable in zebrafish and were possibly hydrolyzed into **3** or **1**. Importantly, these *in vivo* anti-angiogenic data indicate that compound **2** was at least not fully a formal pro-drug of **3** or **1** in zebrafish, and ketal **2** exerted *in vivo* anti-angiogenic activity possibly by itself or ketal **2** was maybe metabolized in part or fully in zebrafish into an unknown more active intermediate(s) than **3** and **1**.

Determination of *in vitro* anti-angiogenic activity with HUVECs

Endothelial cell proliferation is the first step in angiogenesis. Therefore, blocking endothelial cell proliferation will disrupt the progress of angiogenesis.[8] As shown in Fig. 2, Table 2 and Fig. S3 (ESI†), after 48 h of treatment compounds **1**, **2**, **3**, **4**, **5**, **6** and **9** all significantly inhibited VEGF-induced HUVECs proliferation in a dose-dependent manner in their tested range of concentration.

All derivatives of **2**, **3**, **4**, **5**, **6** and **9** showed more potent inhibitory effects on VEGF-induced HUVECs proliferation than their parent compound **1**. In contrast to the inhibition SARs obtained *in vivo* with zebrafish, surprisingly, the inhibitory ability of **3** towards *in vitro* HUVEC proliferation was slightly greater than that of **2**, implying that there is a possibility for **2** to act in part or fully as a pro-drug of **3** or/and **1** in HUVECs. Meanwhile, 14α-ketal **2** showed barely any additional activity against HUVEC proliferation than 14β-ketal **9**, indicating that 14-stereochemistry has no or only a little effect on HUVEC proliferation in the *in vitro* anti-angiogenesis model. Furthermore, no obvious activity difference was observed between 14-acetals **4**, **5** and **6** against HUVEC proliferation, suggesting that 3,19-acetonylidene ketal and 3,19-methylene acetal have no key contribution to the anti-HUVEC proliferative activity. Since the inhibitory activities of three 14-acetals (**4**, **5** and **6**) towards HUVEC proliferation were stronger than those of 14α-ketals **2** and **9**, it seems that the spatial hindrance of the ketals negatively affects their anti-HUVEC proliferative activities; however, similar results originating from the hindrance of ketals were not found in the aforementioned *in vivo* anti-angiogenesis experiment with zebrafish. Importantly, the SARs of these compounds differed depending on whether their anti-angiogenic activity was evaluated in terms of VEGF-induced HUVEC proliferation or *in vivo* using the zebrafish model.

As endothelial cell migration is a key component of angiogenesis,[8] the effects of these compounds on the basal migration of endothelial cells were investigated using the Transwell Migration Assay (Fig. 3A, S4 and Table S1 in ESI†). Compared with the non-VEGF control, the migratory ability of HUVECs to cross the polycarbonate membrane was stimulated by VEGF (20 ng ml^{-1}). As shown in Table S1 (ESI†), VEGF-stimulated motility of HUVECs was suppressed by these compounds in a dose-dependent manner and 100% motility was inhibited by **2** at 20 μM, by **4**, **5** and **6** at 10 μM, and by **3** and **9** at 25 μM, but **1** inhibited migration by less than 20% at 25 μM. The SARs of these compounds for inhibiting HUVEC migration are almost the same as those for their inhibition of HUVEC proliferation.

Cell invasion is essential for endothelial cells in angiogenesis.[8] Therefore, we performed assays to evaluate the ability of these compounds to inhibit VEGF (20 ng ml^{-1})-stimulated HUVECs from passing through the Matrigel-coated membrane barriers of Transwell. The results are listed in Fig. 3B, Table S1 and Fig. S5 (ESI†), in which all derivatives exerted a stronger inhibitory effect in a concentration-dependent manner on VEGF-stimulated HUVEC invasion than the parent compound **1**. The invasiveness of HUVECs was 100% inhibited by 10 μM of compounds **4**, **5** and **6**, compared to 0% by **1**, 35% by **2**, 60% by **3**, and 60% by **9** at 10 μM. The SARs of these compounds in HUVEC invasion were found to be similar to those in HUVEC proliferation and migration.

Tube formation of HUVECs is a critical step in the process of angiogenesis[8] and we were interested in whether these compounds inhibited the formation of *in vitro* chord-like networks of HUVECs. As shown in Fig. 4, Table S1 and Fig. S6 (ESI†), HUVECs plated on the surface of Matrigel formed capillary-like structures in the vehicle group within 5 h and more chord-like networks were constructed after HUVECs were stimulated with VEGF (20 ng ml^{-1}). As shown in Fig. 4 and Table S1 (ESI†), 25 μM of parent compound **1** inhibited 70% tube formation and the capillary tube was more than 90% suppressed in the presence of 20 μM of **2**, 10 μM of **9**, or 5 μM of **3**, **4**, **5** and **6**. Noticeably, 2.5 μM of **4**, **5** and **6** inhibited the formation of chord-like networks of HUVECs by more than 50%.

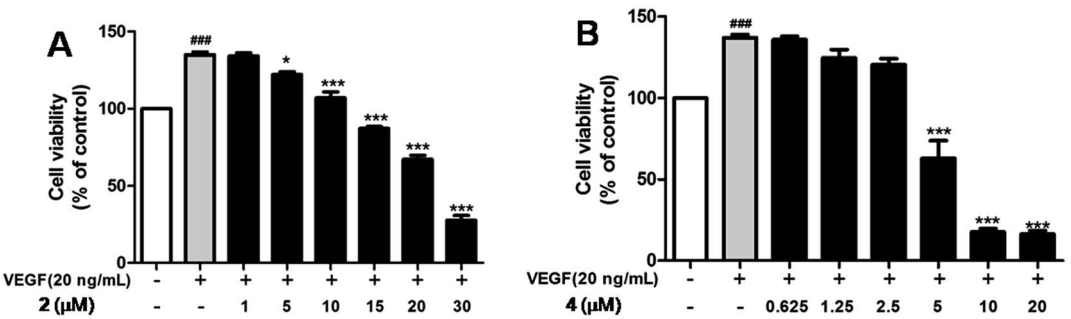

Fig. 2 Effect of **2** (A) on VEGF-induced HUVECs proliferation compared with that of **4** (B).

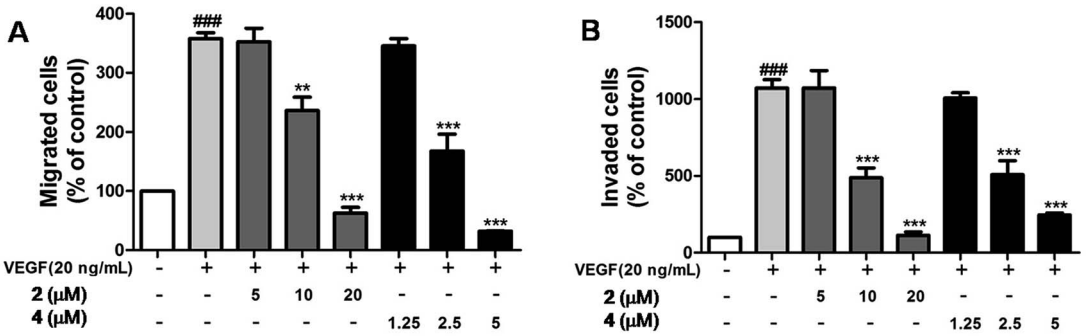

Fig. 3 Effects of 2 on the VEGF-induced HUVECs Transwell migration assay (A) and Transwell invasion assay (B) compared with those of 4.

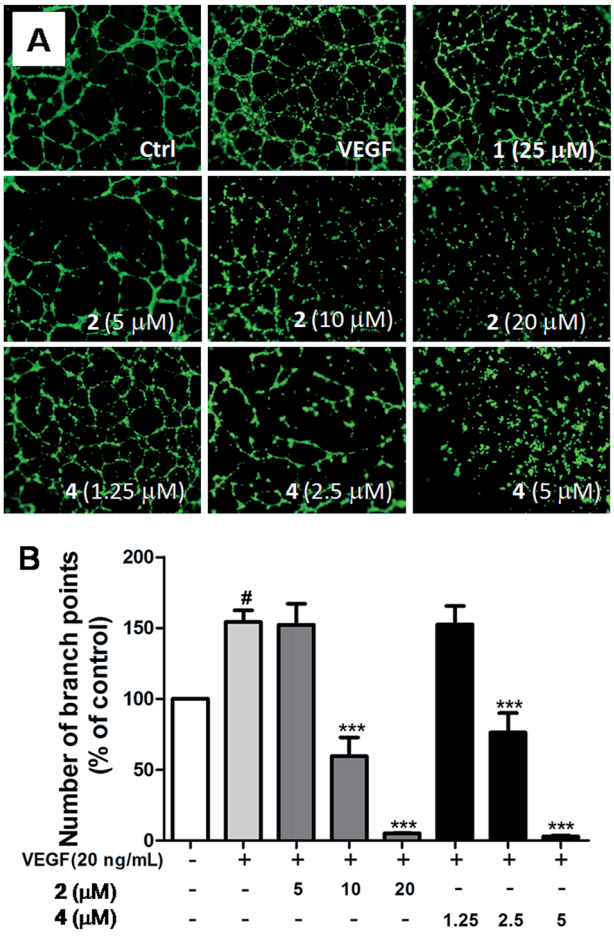

Fig. 4 Effect of 2 on the tube formation of HUVECs compared with 4 (A) and the inhibitory activity of 2 and 4 on tube formation was quantified by determining the number of branch points (B).

These findings demonstrated that the SARs of these compounds in inhibiting tube formation in HUVECs parallel those in the anti-HUVEC proliferation experiment.

As a whole, these data demonstrated that all of these compounds can inhibit the basic processes of *in vitro* angiogenesis including HUVEC proliferation, migration, invasion and tube formation. Interestingly and maybe more importantly, the SARs for the *in vitro* and *in vivo* anti-angiogenesis experiments in HUVECs and zebrafish, respectively, are totally different, with the most active compounds against *in vitro* angiogenesis being **4**, **5** and **6**, and compound **2** being the most potent compound in *in vivo* anti-angiogenesis.

Survival rate of zebrafish and HUVECs viability with 2

Since 14α-ketal compound **2** is more active than the other compounds against the *in vivo* blood vessel formation of zebrafish, the survival rate of zebrafish and the cell viability of HUVECs treated with **2** were studied.

The beating heart of the zebrafish embryo is a common and direct parameter that indicates the living status of embryos and can be used to determine survival rate or mortality. Thus, the number of embryos with a heartbeat was determined 0, 8, 12 and 24 hours post treatment (hpt) after treatment with **2**. As shown in Fig. 5A, embryos treated with 100 μM of **2** exhibited mild toxicity at 8 hpt, and this toxicity gradually increased with zero survival of embryos at 24 hpt. However, most of the zebrafish embryos were alive after 24 h when treated with the lower doses of 30 and 10 μM of **2**. As the IC_{50} value of **2** for *in vivo* anti-angiogenesis in zebrafish is 32.4 ± 2.5 μM, the toxicity to zebrafish is relatively low at 24 hpt.

An MTT assay was performed to determine HUVEC viability after treatment with **2** for 24 h. As shown in Fig. 5B, **2** induced increasing cytotoxicity in a dose-dependent manner in the concentration range 5–30 μM and its CC_{50} value to HUVECs was 28.1 ± 1.5 μM. When the applied concentration of **2** was lower than 20 μM, **2** was found to be almost non-toxic to HUVECs. However, at 25 μM **2** showed mild cytotoxicity and at 30 μM HUVEC viability decreased to less than 50%, indicating that the cytotoxicity is in a reasonable range.

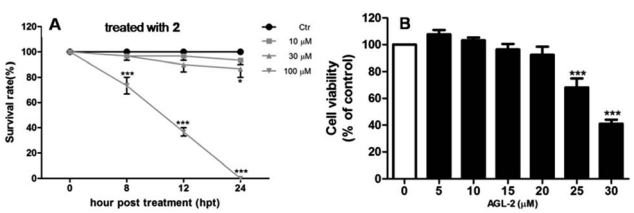

Fig. 5 Effects of 2 on the survival rate (A) of zebrafish and cell viability (B) of HUVECs.

Effects of 2 on the expression and phosphorylation of proteins involved in the angiogenesis signaling pathway in HUVECs

In order to decipher how **2** inhibits angiogenesis, the underlying molecular mechanisms of **2** in VEGF (50 ng ml^{-1})-stimulated HUVECs were investigated by detecting the expression and phosphorylation of key proteins in angiogenesis by Western blotting (Fig. 6). Since less than 20 μM of **2** is almost non-toxic to HUVECs, the HUVECs were treated with 5, 10 and 20 μM of **2** for 4 h before being exposed to VEGF (50 ng ml^{-1}) for 15 min. It was firstly discovered that the phosphorylation of VEGFR2 in VEGF-activated HUVECs was dose-dependently down-regulated by **2**. Furthermore, the phosphorylation of several proteins (Akt, MEK, ERK1/2 and Src) that are related to the regulation of angiogenesis was found to be inhibited in a dose-dependent manner and greatly decreased by 20 μM of **2** in VEGF-activated HUVECs; however, the expression levels of *p*-Fak and *p*-mTOR were only slightly decreased. As shown in Fig. 6, there is almost no change in the expression of the proteins VEGFR2, Akt, MEK, ERK1/2, Src, Fak and mTOR after the treatment with gradient concentrations of **2**. These results demonstrated that the mode of anti-angiogenic action by **2** is associated with blocking the phosphorylation of the VEGF/VEGFR2 angiogenesis signaling pathway.

The stability of 2 and 4 in HUVEC and zebrafish media: providing insight into the difference in anti-angiogenic activity *in vitro* and *in vivo*

It is expected that a typical pro-drug decomposes into its parent drug after it is present in zebrafish or HUVECs. However, it is also possible for a modified compound to possess better properties in some aspects for drug application than its parent drug, *e.g.* better solubility, even though it will be decomposed in part before being absorbed by zebrafish or HUVECs. Under such circumstances, a potential pro-drug may perform its function *in vivo* or *in vitro* by metabolized structures and the efficacy of this kind of pro-drug could come from a pro-drug itself (intact), parent drugs (decomposed) or metabolites in zebrafish or in HUVECs.

HPLC analysis of the stability of **2** and **4** incubated in HUVEC medium and zebrafish medium for different time periods was conducted and the results are shown in Fig. S7–S11 (ESI†). According to Fig. S7a and b,† a final concentration of 20 μM of **2** or **4** was applied for incubation with HUVEC medium or zebrafish medium for feasible HPLC analysis. In a general mode, the predictable decomposition products of **2** and **4** are **3** or/and **1**. As shown in Fig. S8,† **2** (RT ~ 18.5 min) was not stable for a long time in HUVEC medium, but it was not decomposed completely in 22 h (Fig. S8i and j†). Since none of **3** (RT ~ 8.5 min) was observed in HUVEC medium (Fig. S8†), **1** should be formed. However, **1** (RT ~ 4.5 min) was overlapped with

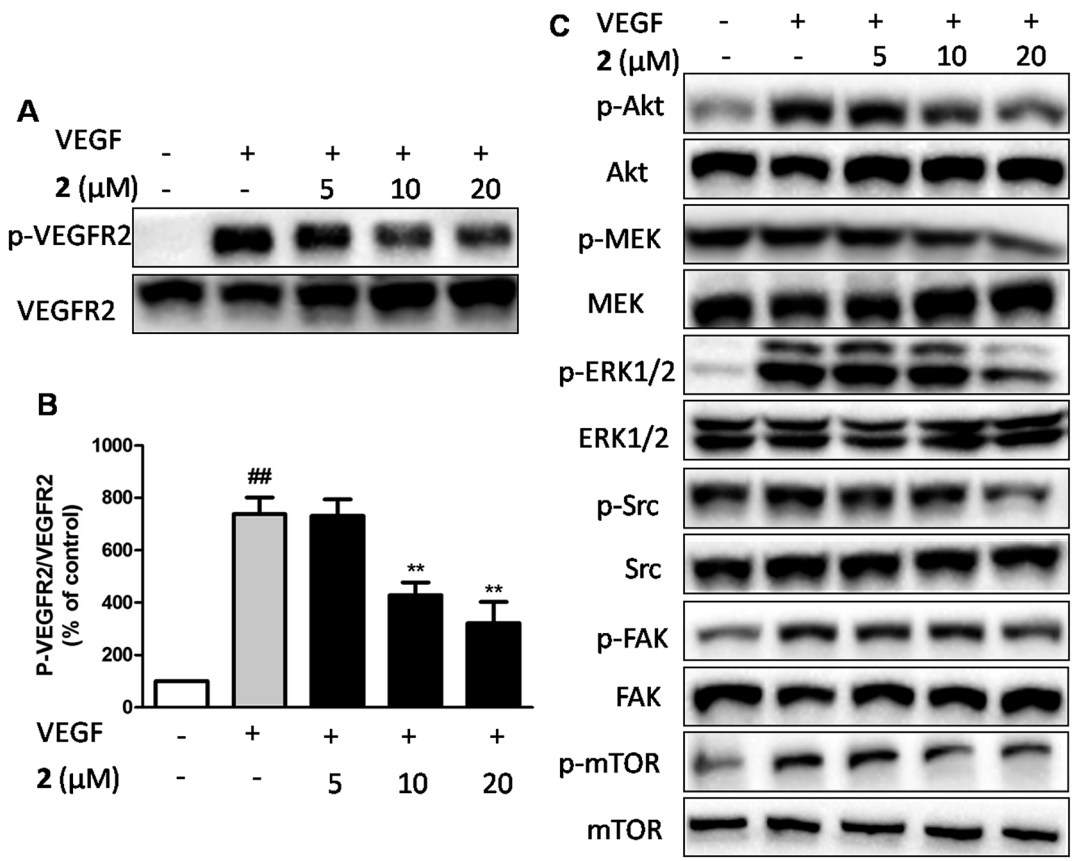

Fig. 6 Effects of **2** on the expression of VEGFR2 and its phosphorylation (A and B) and VEGFR2-mediated downstream signaling (C).

component(s) of HUVEC medium (Fig. S8†), which could not be avoided. Because the IC_{50} value of **2** against HUVEC proliferation is slightly higher than that of **3** but much lower than that of **1** (Table 2), the observed anti-angiogenic activity of **2** towards HUVECs was quite possibly from absorbed **2** and **1** in HUVECs, in which **2** worked as a pro-drug of **3** or by itself. Similarly, **2** was decomposed gradually in zebrafish medium (Fig. S9†) and a small amount of **2** was left after 21 h (Fig. S9g and h†). On the other hand, none of **1** was obviously observed around 4.5 min (Fig. S9†) but **2** was quantitatively transformed into **3** in zebrafish medium (Fig. S9†). Since the anti-angiogenic activity of **3** is much less than that of **2** in the zebrafish model (Table 2), the contribution of **3** to the anti-angiogenic activity was ignorable. These results suggested that **2** should be absorbed quickly by zebrafish before being decomposed into **3** in zebrafish medium. If **2** were to act as a full pro-drug of **3** or/and **1** in zebrafish, an accumulated concentration of **2** more than three (for **3**) or ten (for **1**) times higher would be required; therefore, it is more likely that **2** worked by itself or its unknown active metabolite(s) in zebrafish.

Even though it is difficult to separate **4** from the media and the peak of **4** (RT $\sim$ 12.8 min) was totally overlapped with component(s) from HUVEC medium (Fig. S10†), it is perceptible from the integrated area by comparing Fig. S10 with Fig. S7c and d.† From analyzing Fig. S10,† it was discovered that **4** was also not stable for a long time in HUVEC medium, while **3** was not obviously observed and **1** should have formed and overlapped with component(s) of HUVEC medium. These findings are coincident with those for **2** in HUVEC medium. Considering that **4** is the most active compound against HUVEC proliferation (Table 2) and **1** is much less active than **4**, the observed activity of **4** was most likely from **4** largely being absorbed by HUVECs before it degrading in the HUVEC medium. Furthermore, the action of **4** appears to be caused by itself or/and an unknown active metabolite(s) in HUVEC and it is not a pro-drug of **1** or **3**. On the other hand, the results from Fig. S11† revealed that **4** was stable in zebrafish medium and neither **1** nor **3** was observed. Even though **4** possibly acted by itself in zebrafish, it is also possible that **4** worked as a pro-drug of **3** in zebrafish in view of the similar IC_{50} values of **3** and **4** against zebrafish development (Table 2).

It can be concluded from these results that compound **4** is stable in zebrafish medium and possibly acts as a normal pro-drug in the zebrafish model. Meanwhile, **2** is not stable for a long time in HUVEC medium and zebrafish medium and **4** is unstable in HUVEC medium, but **2** is much more active than **1** and **3** against zebrafish development and **4** is the most active compound against HUVEC proliferation. This illustrates that **2** (by HUVECs and zebrafish) and **4** (by HUVECs) are absorbed much more quickly than they are decomposed in the media.

SARs differentiating the tested compounds' *in vitro* and *in vivo* anti-angiogenic activity

Through the aforementioned comparisons, some important factors affecting these compounds' *in vitro* and *in vivo* anti-angiogenesis SARs with HUVECs and zebrafish, respectively, were discovered. Firstly, the stabilities of ketal **2** and acetal **4** are very similar in HUVEC medium but **2** is much less active in the HUVEC model than **4**, suggesting that the spatial hindrance of the ketal negatively affects the compound's *in vitro* anti-angiogenic activity towards HUVECs. This is possibly due to ketal **2**'s impaired target-binding or/and the chemically less stable 14-ketal moiety of **2**. In contrast, 14-ketal **2** was discovered to be the most active compound in the zebrafish model and much more active than **4**, revealing the positive influence of the hindered ketal on *in vivo* anti-angiogenesis in zebrafish. Importantly, the result that **2** is much more active than **9** in the zebrafish model is attributed to 14-stereochemistry. Secondly, methylene acetals **4**, **5** and **6** were more active than **1**, **2**, **3** and **9** in the HUVEC model, suggesting that the methylene acetal group is more stable in HUVECs than the ketal group. On the other hand, **4** and **5** possessed similar activity to **3** and were less active than ketal **2** in the zebrafish model. Therefore, it is possible for **4** and **5** to act as pro-drugs of **3** in the zebrafish model; the methylene acetals (with less hindrance) were biologically more vulnerable in the zebrafish model than the ketal (with more hindrance) causing 14-acetals **4** and **5** to be quickly decomposed (hydrolyzed) into **3**. Based on the above hypothesis, it is plausible that the much less active compound **6** with a 3,19-acetal and 14-acetal was much more easily hydrolyzed in zebrafish into parent compound **1**, causing compounds **6** and **1** to exhibit similar *in vivo* anti-angiogenic activity in the zebrafish model. Thirdly, **2** and **4** exhibit better anti-angiogenic activity than parent compounds **1** and **3**, indicating that a simple decomposition mode is not the full reason for the activity improvement. Even though a tested compound (*e.g.* **2** or **4**) is not very stable in media, its enhanced lipo-solubility possibly improves its cell permeability, allowing the tested compound to accumulate more quickly and to even higher concentrations in zebrafish or HUVECs, which increases its activity. Therefore, the pro-drug strategy of enhancing lipo-solubility can feasibly improve the convenience of applying very poor water- and lipo-soluble andrographolide (**1**) as a drug and enhance its anti-angiogenic activity. Finally, the difference in anti-angiogenic activity *in vitro* and *in vivo* for HUVECs and zebrafish, respectively, indicates that (in the HUVEC model) **2** probably acts in part or fully as a pro-drug of **3** but **4** is not a typical pro-drug of **1** or **3** and it is more probable that it exerts its action by itself or/and its unknown active metabolite(s). By contrast, in the zebrafish model, it is more likely that **4** is a typical pro-drug of **3**, while **2** is not a typical pro-drug of **3** or **1** and it induces *in vivo* anti-angiogenic effects by itself or/and its unknown active metabolite(s).

Conclusions

In summary, a series of acetal and ketal derivatives of andrographolide were synthesized. Even though their "Rule of Five" properties, including clog *P*, are poorer than those of **1**, these compounds have better lipo-solubility than the parent compound andrographolide (**1**), which possesses very poor water-solubility and lipo-solubility. It was discovered that these compounds exhibited better angiogenesis inhibitory activity

than **1** for *in vivo* and *in vitro* anti-angiogenesis in the zebrafish and HUVEC models, respectively. Interestingly, these compounds' SARs differed between the HUVEC and zebrafish models, with 14α-ketal **2** showing the best *in vivo* anti-angiogenesis activity to zebrafish, while 14α-acetals **4**, **5** and **6** were more active than the other compounds and **1** for *in vitro* anti-angiogenesis with HUVECs. In addition, 14-stereochemistry is important for *in vivo* anti-angiogenesis in zebrafish, with the result that **2** is much more active than **9** in the zebrafish model. The anti-angiogenic activity of these ketal and acetal derivatives may benefit from their enhanced lipo-solubility improving their cell permeability, allowing them to be quickly absorbed by HUVECs or zebrafish and even increasing their observed concentration in zebrafish and HUVECs. Also, the better anti-angiogenic activity of **2** and **4** than **1** potentially results from their active metabolite(s) in zebrafish or HUVECs. These data suggested that rational modifications improve the practicality of **1** and the stability of these compounds were affected by the *in vitro* and *in vivo* model systems, which possibly differentiated their anti-angiogenic activities to engender different pharmacological outcomes. Moreover, the underlying molecular mechanisms of compound **2**'s action were disclosed, with VEGF-stimulated angiogenesis being significantly inhibited by compound **2** *via* targeting the phosphorylation of VEGFR2 and VEGFR2-mediated downstream angiogenesis signaling pathways.

Although these compounds are not potent enough in their current forms and have shortcomings in stability, these acetal and ketal derivatives of andrographolide are promising lead compounds for further evaluation in the treatment of anti-angiogenesis. Therefore, our efforts to design and synthesize more potent and stable acetal and ketal derivatives of andrographolide and exploit their action mechanisms are actively continuing in our laboratories.

Experimental

Materials and equipment for chemistry

Unless otherwise stated, materials were obtained from commercial suppliers and used without further purification. ^{1}H and ^{13}C NMR spectra were recorded on a Bruker AV-400 spectrometer at 400 and 101 MHz, respectively, in an indicated deuterated solvent. Coupling constants (J) are expressed in hertz (Hz). NMR chemical shifts (δ) are reported in parts per million (ppm) units relative to the solvent. High resolution mass spectrometry (HRMS) was performed using an Applied Biosystems Q-STARElite ESI-LC-MS/MS mass spectrometer. Melting points were measured using an YRT-3 melting point apparatus (Shanghai, China) and were uncorrected. HPLC conditions for the purification of **2**, **4**, **5**, **6** and **9**: C18 Sunfire column (4.6 × 250 mm, 5 μm), washed by 80% methanol with 20% purified water, rate = 0.8 ml min^{-1}, detection wavelength of 220 nm. HPLC conditions for evaluating the stability of **2** and **4** in HUVEC medium and zebrafish medium: C18 Phenomenex Gemini column (4.6 × 250 mm, 5 μm), washed by 80% methanol with 20% purified water, rate = 0.8 ml min^{-1}, detection wavelengths of 220 and 254 nm.

Preparation of 3,19-acetonylidene-14α-(2-methoxypropan-2-yloxy)andrographolide (2), 3,19-acetonylidene andrographolide (3),[4h] 3,19-acetonylidene-14β-(2-methoxypropan-2-yloxy) andrographolide (9) and 3,19-acetonylidene 14β-andrographolide (10).[4h]

Method A. Modified from ref. 4*h*, briefly, 1.0 equiv. of **1** or **8** was dissolved in 5.8 equiv. of dimethoxypropane (DMP) and dry dichloromethane (DCM) (DCM/DMP (v/v) = 1/2). After 10 equiv.% of pyridinium *p*-toluenesulfonate (PPTS) was added, the reaction mixture was stirred at 45 °C for about 3 h and the reaction progress was monitored by TLC. The reaction residue was purified by silica gel chromatography (petroleum ether (PE)/ethyl acetate (EA) 7/1) to give about 4% yield of **2** and (PE/EA 3/1) 93% yield of **3**, and 3% yield of **9** and 90% yield of **10**. Compound **2** (HPLC purity ≧ 98%): white solid; mp 78.3–79.7 °C; ^{1}H NMR (400 MHz, C_6D_6) δ 7.03 (m, 1H), 4.87 (s, 1H), 4.75 (s, 1H), 4.68–4.61 (m, 1H), 3.96 (dd, J = 9.9, 3.7 Hz, 1H), 3.91 (dd, J = 9.8, 6.3 Hz, 1H), 3.86 (d, J = 11.7 Hz, 1H), 3.49 (dd, J = 7.3, 3.0 Hz, 1H), 3.11 (d, J = 11.5 Hz, 1H), 2.88 (s, 3H), 2.59 (m, 1H), 2.20 (m, 2H), 1.96–1.83 (m, 1H), 1.76 (m, 1H), 1.67–1.55 (m, 2H), 1.51 (d, J = 11.2 Hz, 1H), 1.45 (s, 3H), 1.41 (s, 3H), 1.35 (m, 1H), 1.18 (s, 3H), 1.10 (s, 3H), 1.07 (s, 4H), 1.02 (dd, J = 12.8, 4.1 Hz, 1H), 0.97 (s, 3H), 0.96–0.92 (m, 1H); ^{13}C NMR (101 MHz, C_6D_6) δ 169.2, 147.7, 147.2, 126.9, 109.6, 101.5, 99.6, 75.3, 72.2, 66.8, 64.4, 56.1, 51.2, 49.5, 38.4, 38.3, 37.9, 34.2, 26.5, 26.1, 25.3, 25.0^{1}, 24.9^{7}, 24.8, 24.7, 23.4, 17.0; HRMS (ESI) m/z: 485.2872 $[M + Na]^+$, calculated for $C_{27}H_{42}O_6Na$, 485.2879. Compound **9** (HPLC purity ≧ 95%): white solid; mp 121.6–123.4 °C; ^{1}H NMR (400 MHz, C_6D_6) δ 7.01 (m, 1H), 4.88 (s, 1H), 4.74–4.64 (m, 1H), 4.48 (s, 1H), 4.02 (dd, J = 10.0, 3.1 Hz, 1H), 3.88–3.79 (m, 2H), 3.47 (dd, J = 7.2, 3.0 Hz, 1H), 3.10 (d, J = 11.5 Hz, 1H), 2.89 (s, 3H), 2.52–2.41 (m, 1H), 2.33 (m, 1H), 2.20 (m, 1H), 1.90–1.77 (m, 1H), 1.72 (m, 1H), 1.59–1.50 (m, 2H), 1.50–1.45 (m, 1H), 1.44 (s, 3H), 1.40 (s, 3H), 1.34 (m, 1H), 1.17 (s, 3H), 1.08 (s, 3H), 1.06 (s, 3H), 1.05–1.00 (m, 2H), 0.98 (s, 3H), 0.87 (dd, J = 12.9, 2.6 Hz, 1H); ^{13}C NMR (101 MHz, C_6D_6) δ 169.4, 148.3, 147.1, 127.1, 108.3, 101.5, 99.6, 75.2, 72.2, 67.1, 64.4, 55.7, 51.0, 49.5, 38.4, 38.3, 37.8, 34.0, 26.4, 26.0, 25.3, 25.2, 25.1, 24.7^{4}, 24.6^{6}, 23.4, 17.0; HRMS (ESI) m/z: 485.2873 $[M + Na]^+$, calculated for $C_{27}H_{42}O_6Na$, 485.2879.

Method B. A method similar to "Method A" was used but 14 equiv. of DMP and corresponding DCM (2/5 (v/v) of DCM/DMP) were used to afford **2** or **9**, and **3** or **10** in yields of about 40% and 56%, respectively.

Method C. A method similar to "Method A" was used but 28 equiv. of DMP was used as a reactant and a solvent and no DCM was used. The reactions gave **2** or **9**, and **3** or **10** in yields of about 38% and 48%, respectively.

Preparation of 3,19-acetonylidene-14α-(2-methoxymethoxy) andrographolide (4). 600 mg (1.54 mmol) of **3** was dissolved in 20 ml dry dichloromethane under N_2 atmosphere. After the solution was cooled in an ice-water bath, 1.5 ml (9.24 mmol) of *N*,*N*-diisopropylethylamine (DIPEA) and 0.59 ml (7.7 mmol) of chloromethyl methyl ether (MOMCl) were added sequentially. The reaction mixture was stirred at 0 °C for 20 min and then at 35 °C for 50 h. Treated with ethyl acetate and brine, the organic

phase was dried over anhydrous Na_2SO_4. Filtered and evaporated, the residue was purified by silica gel chromatography (PE/EA 5/1) to afford 450 mg of **4** (67% yield, HPLC purity ≧ 98%): white solid; mp 117–119 °C; ^{1}H NMR (400 MHz, C_6D_6) δ 7.12–7.06 (m, 1H), 4.85 (flat s, 1H), 4.64 (flat s, 1H), 4.42 (m, 1H), 4.30 (d, J = 7.1 Hz, 1H), 4.22 (d, J = 7.1 Hz, 1H), 3.92 (dd, J = 10.3, 1.9 Hz, 1H), 3.84 (d, J = 11.5 Hz, 1H), 3.78–3.70 (m, 1H), 3.48 (dd, J = 7.5, 3.1 Hz, 1H), 3.09 (d, J = 11.5 Hz, 1H), 3.02 (s, 3H), 2.46–2.35 (m, 1H), 2.34–2.24 (m, 1H), 2.21–2.13 (m, 1H), 1.92–1.85 (m, 1H), 1.78–1.67 (m, 1H), 1.66–1.54 (m, 2H), 1.52–1.46 (m, 1H), 1.47 (s, 3H), 1.40 (s, 3H), 1.37–1.29 (m, 1H), 1.10 (s, 3H), 1.07–0.97 (m, 2H), 0.96–0.88 (m, 4H); ^{13}C NMR (101 MHz, C_6D_6) δ 169.0, 148.0, 147.3, 126.4, 109.1, 99.4, 95.1, 75.3, 71.2, 71.0, 64.2, 55.9, 55.6, 51.3, 38.2, 38.2, 37.7, 34.1, 26.5, 26.0, 25.3, 25.2, 24.8, 23.2, 16.5; HRMS (ESI) m/z: 457.2560 $[M + Na]^+$, calculated for $C_{25}H_{38}O_6Na$, 457.2566.

Preparation of 3,19-acetonylidene-14α-(benzyloxymethoxy) andrographolide (5). 1.5 g (1.54 mmol) of **3** was dissolved in 30 ml dry dichloromethane under N_2 atmosphere and then the solution was cooled in an ice-water bath. After 3.8 ml (23.1 mmol) of DIPEA and 2.7 ml (19.25 mmol) of chloromethyl benzyl ether (BOMCl) were added sequentially, the reaction mixture was stirred at 0 °C for 20 min and at 35 °C for 48 h. Treated with ethyl acetate and brine, the organic phase was dried over anhydrous Na_2SO_4. Filtered and evaporated, the residue was purified by silica gel chromatography (PE/EA 6/1) to afford 1.2 g of **5** (61% yield, HPLC purity ≧ 98%): white solid; mp 126–128 °C; ^{1}H NMR (400 MHz, C_6D_6) δ 7.24–7.16 (m, 4H), 7.15–7.05 (m, 2H), 4.84 (flat s, 1H), 4.63 (flat s, 1H), 4.50 (m, 1H), 4.46 (m, 1H), 4.40 (m, 1H), 4.38 (s, 2H), 3.99 (dd, J = 10.3, 1.6 Hz, 1H), 3.83 (m, 1H), 3.75 (m, 1H), 3.46 (dd, J = 8.0, 3.4 Hz, 1H), 3.10 (d, J = 11.5 Hz, 1H), 2.44–2.27 (m, 2H), 2.21–2.13 (m, 1H), 1.91–1.79 (m, 1H), 1.77–1.66 (m, 1H), 1.61–1.48 (m, 2H), 1.45 (s, 4H), 1.40 (s, 3H), 1.38–1.29 (m, 1H), 1.11 (s, 3H), 1.05–0.87 (m, 3H), 0.83 (s, 3H); ^{13}C NMR (101 MHz, C_6D_6) δ 169.1, 148.1 (2C), 147.3 (2C), 137.8, 128.6, 128.0, 127.8, 126.4, 109.0, 99.3, 92.9, 75.5, 71.3, 71.0, 69.9, 64.1, 55.8, 51.4, 38.3, 38.1, 37.7, 34.2, 26.8, 26.1, 25.3^2, 25.2^7, 24.9, 23.1, 16.3; HRMS (ESI) m/z: 533.2875 $[M + Na]^+$, calculated for $C_{31}H_{42}O_6Na$, 533.2879.

Preparation of 3,19-methylene acetal-14α-(methoxymethoxy) andrographolide (6). To the solution of 500 mg (1.28 mmol) of **3** in 20 ml dichloromethane under N_2 atmosphere, 2.13 ml (15.4 mmol) of TEA and 1.0 ml (12.8 mmol) of MOMCl was added sequentially. The reaction mixture was stirred at room temperature for 12 h. Treated with ethyl acetate, sat. sol. $NaHCO_3$ and brine, the organic phase was dried over anhydrous Na_2SO_4. Filtered and evaporated, the residue was purified by silica gel chromatography (PE/EA 3/1) to afford 450 mg of **6** (86% yield, HPLC purity ≧ 98%): white solid; mp 131–133 °C; ^{1}H NMR (400 MHz, C_6D_6) δ 7.05 (td, J = 6.8, 1.7 Hz, 1H), 4.93 (d, J = 6.3 Hz, 1H), 4.79 (d, J = 6.4 Hz, 2H), 4.61 (s, 1H), 4.42 (d, J = 5.7 Hz, 1H), 4.32 (d, J = 7.1 Hz, 1H), 4.23 (d, J = 7.1 Hz, 1H), 3.94 (dd, J = 10.3, 2.0 Hz, 1H), 3.86–3.72 (m, 2H), 3.42 (dd, J = 12.8, 4.5 Hz, 1H), 3.32 (d, J = 11.2 Hz, 1H), 3.03 (s, 3H), 2.35–2.17 (m, 2H), 2.15–1.97 (m, 2H), 1.74–1.62 (m, 1H), 1.54–1.45 (m, 2H), 1.46 (s, 3H), 1.41–1.35 (m, 2H), 0.88–0.70 (m, 3H), 0.53 (s, 3H); ^{13}C NMR (101 MHz, C_6D_6) δ 168.9, 147.8, 147.0, 126.4, 109.2, 95.2, 87.8, 79.2, 71.3, 71.1, 68.9, 55.6, 55.4, 54.5, 38.7, 37.6 (2C), 35.8, 26.1, 24.8, 22.5, 21.2, 15.1; HRMS (ESI) m/z: 429.2244 $[M + Na]^+$, calculated for $C_{23}H_{34}O_6Na$, 429.22531.

HPLC analysis of the stability of 2 and 4 in HUVEC medium and zebrafish medium

In order to cover **1**, **2** and **3** or **1**, **3** and **4** in one HPLC spectrum, it is inevitable that the peaks of **1** and **4** will overlap with some components of HUVEC medium under the optimal HPLC analysis conditions, since the components of HUVEC medium are very complicated (Fig. S7c and d†). Concentrations of **1**, **2**, **3** and **4** in the reference solution (Fig. S7a and b†) were about 10, 20, 20 and 20 μM, respectively. Accordingly, in order to get useful information, the final concentrations of **2** and **4** were set to 20 μM in both media. Compounds **2** and **4** were prepared in 20 mM stock solution in methanol and 1 μl of 20 mM stock solution was added to 1 ml medium to produce a 20 μM final concentration of **2** or **4**. Each HUVEC medium sample was filtered through a 0.22 μm pore filter before HPLC injection, while the zebrafish medium sample was injected directly. Each injection volume was 20 μl.

The results at dual wavelengths of 220 and 254 nm are presented in Fig. S7–S11† for comparison since the maximum absorbance wavelengths of the andrographolide skeleton are at 220 and 254 nm.

Assay reagents and handling of compounds

Vascular endothelial growth factor (VEGF) was bought from R&D System (Minneapolis, MN) and VEGFR tyrosine kinase inhibitor II (VRI, Cat. no. 676481) was obtained from CalBiochem (USA). Andrographolide was obtained from Nanjing Chemlin Chemical Industry Co. Ltd. (Nanjing, China). Kaighn's Modification of Han's F12 medium (F-12K), fetal bovine serum (FBS), phosphate-buffered saline (PBS), penicillin–streptomycin (P/S), and 0.25% (w/v) trypsin/1 mM EDTA were purchased from Invitrogen (Carlsbad, CA, USA). Endothelial cell growth supplement (ECGS), heparin, collagen, dimethyl sulfoxide (DMSO), protease and 3-(4,5-dimethylthiazol-2-yl)-2,5-diphenyltetrazoliumbromide (MTT) were purchased from Sigma Aldrich Company (St. Louis, MO). Growth factor reduced (GFR) Matrigel™ were supplied by BD Biosciences (Bedford, MA). Antibodies against Akt, phospho-Akt, Erk1/2, phosphor-Erk1/2, Src, phosphor-Src, MEK, phosphor-MEK, Fak, phospho-Fak, phosphor-VEGFR2 and β-actin were all purchased from Cell Signaling Technology (Danvers, MA).

All compounds including andrographolide (**1**) and VRI were dissolved in DMSO as 100 mM stock solutions. The stock solutions were diluted into different concentrations depending on the assay. All stock solutions were freshly prepared or stored at −20 °C before use. The final concentration of DMSO in each well was 0.1% for the HUVEC assay or 1% for the zebrafish assay.

HUVECs

Human umbilical vein endothelial cells (HUVECs) were obtained from Invitrogen (CA, USA). HUVECs were cultured in F-

12K complete medium with 100 μg ml^{-1} heparin, 30 μg ml^{-1} ECGS, 10% heat-inactivated FBS and 1% P/S. Cells were incubated at 37 °C in a humidified atmosphere with 5% CO_2. Early passage cells (3–8 passages) were used in all assays. Tissue flasks pre-coated with 0.2% collagen were used.

Cell viability assay

HUVECs were seeded into a 96-well plate at a density of 10^5 cells per ml in F-12K complete medium for 24 h to achieve attachment. Then, cells were starved with low serum medium (0.5% FBS) overnight to achieve a quiescent state. After starvation, cells were treated with various concentrations of tested compounds for 24 h. Cell viability was assessed by MTT assay as described by the manufacturer's protocol. Each experiment was repeated three times independently.

Cell proliferation assay

HUVECs were seeded into a 96-well plate at a density of 10^5 cells per ml in F-12K complete medium for 24 h to achieve attachment and confluence. Then, cells were starved with low serum medium (0.5% FBS) overnight to achieve a quiescent state. After starvation, cells were treated with various concentrations of tested compounds in low serum medium (0.5% FBS) containing VEGF (20 ng ml^{-1}) for 24 h. Cell viability was assessed by MTT assay as described by the manufacturer's protocol. Each experiment was repeated three times independently.

Cell migration and invasion assay

The effect of the tested compounds on HUVECs migration and invasion was examined using the transwell system, which consists of a 10 mm tissue culture insert (transwell) with a polycarbonate membrane (8 μm pores) and a 24-well companion plate. In the migration assay, the upper and lower sides of the membrane were pre-coated with 0.2% collagen for 1 h. In the invasion assay, the upper and lower sides of the membrane were pre-coated with 1 : 30 (v/v) and 1 : 100 (v/v) of Matrigel (BD Biosciences, USA), respectively. HUVECs (2.5×10^5 cells per ml) were resuspended in 200 μl low serum (0.5% FBS) medium containing VEGF (20 ng ml^{-1}) and different concentrations of tested compounds. Inserts were then deposited into the 24-well companion plate with 500 μl low serum (0.5% FBS) medium containing 20 ng ml^{-1} VEGF and different concentrations of tested compounds to the upper sides, and the transwell systems were incubated at 37 °C for 24 h. Cells on the upper surface of the membrane were removed using cotton swabs. The inserts were fixed with 4% paraformaldehyde for 15 min, and then mounted on microscope slides after staining with Hoechst 33342 (10 μg ml^{-1}) for 15 min. Images of the cells were captured at 4× magnification using a fluorescent inverted microscope and a CCD camera. HUVECs migration and invasion was quantified by counting the number of cells per insert using Image J. Each sample was assayed in duplicate, and three independent experiments were performed.

Chord-like network structures assay

Matrigel matrix (BD, Biosciences) was thawed at 4 °C overnight. A 15-well μ-slide angiogenesis plate was coated with 10 μl Matrigel per well and incubated at 37 °C for 30 min for polymerization. HUVECs (2.5×10^5) were resuspended in 50 μl medium (0.5% FBS) containing 20 ng ml^{-1} VEGF and different concentrations of tested compounds, and seeded onto the Matrigel-coated plate. After 4–6 h incubation, cells were stained with calcein AM (2 μg ml^{-1}). HUVECs in the vehicle control group formed a tube-like structure, which were defined as endothelial tube formations that connected at both ends. Images were captured at 4× magnification using a fluorescent inverted microscope (Axiovert 200, Carl Zeiss, HK) and a CCD camera (AxioCam HRC, Carl Zeiss, HK). The formation of chord-like networks was quantified by counting the number of branching points in three randomly selected fields.

Zebrafish maintenance and embryo handling

All animal experiments were conducted according to the ethical guidelines of Institute of Chinese Medical Science (ICMS), University of Macau and the protocol was approved by ICMS, University of Macau. Transgenic zebrafish *Tg(fli1a:EGFP)*, which express enhanced green fluorescent protein (GFP) in all endothelial cells, were provided by Zebrafish Information Research Center (ZIRC, Oregon, USA). Wild-type (WT) zebrafish were purchased from a local pet shop. Both strains of zebrafish were maintained as described in the Zebrafish Handbook. In brief, zebrafish were kept separately with a 14/10 h light/dark cycle under standard conditions at 28.5 °C and fed twice a day with brine shrimp and occasionally general tropical fish food. Zebrafish embryos were generated by natural pairwise mating and were collected to be raised in embryo medium at 28.5 °C incubator. Any dead, unfertilized or abnormally hatched embryos were picked out at 4 hours post-fertilization (hpf). 24 hpf embryos were dechorionated by protease in a Petri dish prior to drug treatment and then distributed into a multi-plate with 12 embryos in each group, depending on the assay.

Toxicity of 2 and survival of zebrafish

24 hpf wild-type zebrafish embryos were placed in a 24-well plate. 12 Embryos per well were incubated with 1 ml embryo medium containing various concentrations of the tested compounds at 28 °C for 24 h. At 8 hpt, 12 hpt and 24 hpt, embryos were observed for survival rate. Each experiment was repeated at least three times.

Zebrafish embryo morphological observations

24 hpf *Tg(fli-1a:EGFP)* zebrafish embryos were distributed in a 12-well plate with 12 embryos per group. Each group was treated with different concentrations of tested compounds dissolved in embryo medium for 12 h. Embryos receiving DMSO (1%) and VRI (250 ng ml^{-1}) served as the vehicle control and positive control, respectively. After drug exposure, embryos were observed for morphological changes in ISV and images were captured at 40× and 100× magnifications using an Olympus

Spinning Disk Confocal Microscope System (IX81 Motorized Inverted Microscope [w/ZDC], IX2 universal control box, X-cite series 120, DP71 CCD Camera). Images were analyzed using Adobe Photoshop 7.0. The number of intact and defective ISVs in each zebrafish embryo was counted and measurements were made at each concentration at least three times.

Western blot assay

HUVECs were starved in low serum medium (0.5% FBS) for 2 h, then pretreated with different concentrations of compound **2** for 4 h before exposure to VEGF (50 ng ml^{-1}) for 15 min. Then, proteins were extracted using RIPA lysis buffer containing 1% PMSF and 1% protease inhibitor. Lysates were centrifuged at 12 500 × *g* for 20 min at 4 °C and the supernatant was collected. Total protein concentrations were determined using the BCA™ Protein Assay kit. An aliquot of protein was subjected to SDS-PAGE, and then electrically transferred onto polyvinylidene difluoride membranes. Subsequently, the membrane was blocked for 1 h with 5% non-fat milk in PBS-0.1% Tween 20 (PBST), and incubated with primary antibodies of Akt, p-Akt, MEK, p-MEK, ERK1/2, p-ERK1/2, Src, p-Src, FaK, *p*-Fak, mTOR and *p*-mTOR, VEGFR2, p-VEGFR2 and β-actin, respectively, at 4 °C overnight. Then, the membrane was incubated with horseradish peroxidase-conjugated secondary antibodies for 1 h at room temperature. After repeated washes with PBS, proteins were visualized using an ECL advanced Western blotting detection kit. Photos of protein bands were taken using Image Lab (Bio-Rad). Densitometry measurements of band intensity in the Western blots were performed using Bio-Rad image 5.1.

Data analysis and statistics

Each experiment was repeated at least three times independently. The mean and standard deviations were compared using a one-way ANOVA test with the following statistical criteria: * $p < 0.05$, significant; ** $p < 0.01$, highly significant; *** $p < 0.001$, extremely significant. All data were presented as mean ± SEM.

Acknowledgements

This work was supported by Natural Science Foundation of China (30973621) and Six Major Talents of Jiangsu Province of China (2014). This work was also supported by Overseas and Hong Kong, Macau Young Scholars Collaborative Research Fund by the National Science Foundation of China (No. 81328025), Macau Science and Technology Development Fund (No. 069/2015/A2 and No. 134/2014/A3), and Research Committee, University of Macau (MYRG2015-00182-ICMS-QRCM, MYRG2016-00129-ICMS-QRCM, MYRG2015-00214-ICMS-QRCM, and MYRG2016-00133-ICMS-QRCM).

Notes and references

1 D. J. Newman and G. M. Cragg, *J. Nat. Prod.*, 2016, **79**, 629–661.

2 (*a*) W. A. Boorsma, *Med's Lands Plant*, 1896, **18**, 63; (*b*) M. K. Gorter, *Recl. Trav. Chim. Pays-Bas*, 1911, **30**, 151–160; (*c*) R. J. C. Kleipool, *Nature*, 1952, **169**, 33–34; (*d*) W. Tang and G. Eisenbrand, *Chinese Drugs of Plant Origin*, Springer Verlag, Berlin, 1992; (*e*) W.-L. Deng, *Zhong Cao Yao Tong Xun*, 1978, **10**, 27–30; (*f*) W.-L. Deng, J. Liu and R. Nie, *Acta Pharmacol. Sin.*, 1980, **15**, 590–597; (*g*) T. Zhang, *Zhongyaocai*, 2000, **23**, 366–368.

3 (*a*) R. N. Chakravarti and D. Chakravarti, *Indian Med. Gaz.*, 1951, **86**, 96–97; (*b*) X. Liu, Y. Wang and G. Li, *Zhongyaocai*, 2003, **26**, 135–138.

4 (*a*) R. S. Chang, L. Ding, G. Q. Chen, Q. C. Pan, Z. L. Zhao and K. M. Smith, *Proc. Soc. Exp. Biol. Med.*, 1991, **197**, 59–66; (*b*) A. Basak, S. Cooper, A. G. Roberge, U. K. Banik, M. Chretien and N. G. Seidah, *Biochem. J.*, 1999, **338**, 107–113; (*c*) X. Jiang, P. Yu, J. Jiang, Z. Zhang, Z. Wang, Z. Yang, Z. Tian, S. C. Wright, J. W. Larrick and Y. Wang, *Eur. J. Med. Chem.*, 2009, **44**, 2936–2943; (*d*) Z. Wang, P. Yu, G. Zhang, L. Xu, D. Wang, L. Wang and X. Zeng, *Bioorg. Med. Chem.*, 2010, **18**, 4269–4274; (*e*) B. Das, C. Chowdhury, D. Kumar, R. Sen, R. Roy, P. Das and M. Chatterjee, *Bioorg. Med. Chem. Lett.*, 2010, **20**, 6947–6950; (*f*) V. Menon and S. Bhat, *Nat. Prod. Commun.*, 2010, **5**, 717–720; (*g*) U. Sirion, S. Kasemsook, K. Suksen, P. Piyachaturawat, A. Suksamrarn and R. Saeeneg, *Bioorg. Med. Chem. Lett.*, 2012, **22**, 49–52; (*h*) Z. Liu, W.-K. Law, D. Wang, X. Nie, D. Sheng, G. Song, K. Guo, P. Wei, P. Ouyang, C.-W. Wong and G.-C. Zhou, *RSC Adv.*, 2014, **4**, 13533–13545; (*i*) Y. Peng, J. Li, Y. Sun, J. Y.-W. Chan, D. Sheng, K. Wang, P. Wei, P. Ouyang, D. Wang, S. M. Y. Lee and G.-C. Zhou, *RSC Adv.*, 2015, **5**, 22510–22526; (*j*) R. Preet, B. Chakraborty, S. Siddharth, P. Mohapatra, D. Das, S. R. Satapathy, S. Das, N. C. Maiti, P. R. Maulik, C. N. Kundu and C. Chowdhury, *Eur. J. Med. Chem.*, 2014, **85**, 95–106.

5 (*a*) D. H. Ausprunk and J. Folkman, *Microvasc. Res.*, 1977, **14**, 53–65; (*b*) J. Folkman, *Annu. Rev. Med.*, 2006, **57**, 1–18.

6 D. Hanahan and J. Folkman, *Cell*, 1996, **86**, 353–364.

7 (*a*) S. Liekens, E. De Clercq and J. Neyts, *Biochem. Pharmacol.*, 2001, **61**, 253–270; (*b*) M. E. Eichhorn, S. Strieth and M. Dellian, *Drug Resist. Updates*, 2004, **7**, 125–138.

8 J. Y. Tang, S. Li, Z. H. Li, Z. J. Zhang, G. Hu, L. C. L. C. Cheang, D. Alex, M. P. M. Hoi, Y. W. Kwan, S. W. Chan, G. P. H. Leung and S. M. Lee, *PLoS One*, 2010, **5**, e11822.

9 N. Ferrara and H. P. Gerber, *Acta Haematol.*, 2001, **106**, 148–156.

10 J. Waltenberger, L. Claesson-Welsh, A. Siegbahn, M. Shibuya and C. H. Heldin, *J. Biol. Chem.*, 1994, **43**, 26988–26995.

11 (*a*) A. A. Lanahan, K. Hermans, F. Claes, J. Kerley-Hamilton, Z. W. Zhuang, F. J. Giordan and M. Simons, *Dev. Cell*, 2010, **18**, 713–724; (*b*) G. Mavria, Y. Vercoulen, M. Yeo, H. Paterson, M. Karasarides, R. Marais and C. J. Marshall, *Cancer Cell*, 2006, **9**, 33–44; (*c*) C. Wheeler-Jones, R. Abu-Ghazaleh, R. Cospedal, R. A. Houliston, J. Martin and I. Zachary, *FEBS Lett.*, 1997, **420**, 28–32.

12 U. Langheinrich, *BioEssays*, 2003, **25**, 904–912.

13 (*a*) N. D. Lawson and B. M. Weinstein, *Dev. Biol.*, 2002, **248**, 307–318; (*b*) K. Norrby, *J. Cell. Mol. Med.*, 2006, **10**, 588–612.

14 D. Alex, E. C. Leong, Z. J. Zhang, G. T. Yan, S. H. Cheng, C. W. Leong, Z. H. Li, K. H. Lam, S. W. Chan and S. M. Lee, *J. Cell. Biochem.*, 2010, **109**, 339–346.

15 (*a*) H. W. Lam, H. C. Lin, S. C. Lao, J. L. Gao, S. L. Hong, C. W. Leong, P. Y. Yue, Y. W. Kwan, A. Y. Leung, Y. T. Wang and S. M. Lee, *J. Cell. Biochem.*, 2008, **103**, 195–211; (*b*) S. J. Hong, J. B. Wan, Y. Zhang, G. Hu, H. C. Lin, S. W. Seto, Y. W. Kwan, Z. X. Lin, Y. T. Wang and S. M. Lee, *Phytother. Res.*, 2009, **23**, 677–686.

16 I. K. Lam, D. Alex, Y. H. Wang, P. Liu, A. L. Liu, G. H. Du and S. M. Lee, *Mol. Nutr. Food Res.*, 2012, **56**, 945–956.

17 (*a*) K. Sheeja, C. Guruvayoorappan and G. Kuttan, *Int. Immunopharmacol.*, 2007, **7**, 211–221; (*b*) Z. Yu, B. Lu, Y. Sheng, L. Zhou, L. Ji and Z. Wang, *Biochim. Biophys. Acta*, 2015, **1850**, 824–831; (*c*) T. Y. Lee, H. H. Chang, C. K. Wen, T. H. Huang and Y. S. Chang, *J. Ethnopharmacol.*, 2014, **158**, 423–430; (*d*) K. Shen, L. Ji, B. Lu, C. Xu, C. Gong, G. Morahan and Z. Wang, *Chem.-Biol. Interact.*, 2014, **218**, 99–106.